Moroccan Journal of Chemistry
ISSN: 2351-812X
http://revues.imist.ma/?journal=morjchem&page=login
Budiawanti & al. / Mor. J. Chem. 10 N°2 (2022) 279-287
DOI: https://doi.org/10.48317/IMIST.PRSM/morjchem-v10i2.32642

Photocatalytic Performance of $CoFe_2O_4$-doped Nickel Synthesized by Sol-gel Route

Sri Budiawanti[1], Wahyu Indah Wijiasih[1], Azizah Nur Safitri[1], Farihun Ni'mah[1], Suharno[1], Dwi Teguh Raharjo[1], Budi Purnama[2]

[1]Physics Education Department, Faculty of Teacher Training and Education, Universitas Sebelas Maret, Jl. Ir. Sutami 36A Kentingan, Jebres, Surakarta, 57126, INDONESIA
[2]Physics Department, Faculty of Mathematics and Natural Sciences Universitas Sebelas Maret, Jl. Ir. Sutami 36A Kentingan, Jebres, Surakarta, 57126, INDONESIA

** Corresponding author:*
sribudiawanti@staff.uns.ac.id
Received 12 April 2022,
Revised 22 May 2022,
Accepted 24 May 2022

Abstract

Samples of Ni-doped $CoFe_2O_4$ nanoparticles (NPs) was synthesized by a sol-gel route to discuss doping effect on the photocatalytic performance. The spinel crystal structure of prepared samples was confirmed by XRD and also the crystalline size was calculated. XRD results show that the resulting nanoparticle crystal system is cubic with Fd-3m space group. Based on Rietveld's analysis, it is known that there is a decrease in the lattice parameters along with the addition of Nickel substitution content. FTIR results show absorption peaks in the octahedral and tetrahedral sites. In the image of the SEM results, it is known that agglomerates and irregularities occur in all samples. M-H curve indicates that saturation magnetization and the coercivity value tends to decrease when doping concentration of nickel was increased. In addition, the photocatalytic performance of cobalt ferrite-doped nickel stated that there was an increase in the degradation of methylene blue dye along with the increase in samples irradiation time. It is also seen that the photocatalyst performance increases with the addition of nickel.

Keywords: *Photocatalytic performance; Cobalt ferrite; Nickel; Sol-gel route*

1. Introduction

The rapid development of industry has an impact on decreasing water quality due to the disposal of waste that is not treated properly [1]. Water quality status is the level of water conditions that indicates polluted conditions or good conditions of a water source within a certain period [2]. Several efforts can be made to maintain water quality, one of which is using photocatalyst [3]. Photocatalysts take advantage of the properties of semiconductor materials which have properties between that of an insulator and a conductor. Several materials have been made as photocatalysts, such as zeolite, rare earth nanoparticles, composite materials, ferrites, and others[4]. Among these, the spinel ferrites have more advantages to be photocatalysts. Cobalt ferrite ($CoFe_2O_4$) is one of indispensable spinel ferrites, significantly for photocatalyst. $CoFe_2O_4$ has several excellent physical properties such as high chemical stability and good mechanical chemical stability [5]. $CoFe_2O_4$ also has a narrow bandgap so it is suitable for a photocatalyst [4]. In addition $CoFe_2O_4$ has been developed as photocatalyst because it is cheaper than other materials. The photocatalytic properties of $CoFe_2O_4$ are highly dependent on the nanocrystalline structure [5]. Crystal structures such as shape, size, and purity of nanoparticles can be used to show their physical properties [6]. The high crystallinity value will minimize interface recombination so as to increase the efficiency of electrons and holes to participate in the photocatalyst reaction [7]. According to [7] transfer of electrons from the valence band can occur through 3 mechanisms, namely: thermal excitation, photoexitation, and doping. Giving doping is a mechanism that has been developed a lot. Doping causes an imbalance that results in oxidation or reduction of the absorbed substrate on the semiconductor surface [8]. On the other hand, the doping of transition metals such as V, Zn, Mo, Ni, Cu, and others can change the physical properties and increase the catalytic function[9]. In this research, $CoFe_2O_4$ was made with Nickel (Ni) doping. Ni-doped $CoFe_2O_4$ will produce a material that has good photocatalytic performance [10]. There were many methods which available for $CoFe_2O_4$ such as Co-precipitation, hydrothermal, combustion route, sol-gel route, etc. Sol-gel route is a method that is widely used because it is simple, low cost, and it can make Nps at low temperatures in a short time. In this research, the Ni-doped $CoFe_2O_4$ NPs was carried out with different weight percentage of Nickel (2wt%, 4wt%, 6wt%, 8wt%, 10wt%) and using the sol-gel route. Total concentration of the materials was 0.4 M. In this paper, we investigate the photocatalytic performance of Ni-doped $CoFe_2O_4$ synthesized by sol-gel route.

2. Experimental

2.1. Materials

The chemicals used to synthesis $CoFe_2O_4$ and Ni-doped $CoFe_2O_4$ NPs were Cobalt (II) nitrat hexahydrate ($Co(NO_3)_2.6H_2O$), Ferrite (III) Nitrate nonahydrate ($Fe(NO_3)_3.9H_2O$), Nickel (II) nitrate hexahydrate ($Ni(NO_3)_3.6H_2O$), Citric Acid ($C_6H_8O_7.H_2O$) and double-distilled water.

2.2. Procedure

All of the materials were mixed in one beaker glass with the use of magnetic stirrer at a speed of 6 rpm. During synthesis, the temperature of the solution was checked periodically and the temperature was kept in the range 80^0-90^0C. The solution was heated until it thickens and turns into a gel. Then the stirrer was stopped when the solution becomes gel and the gel was stirred manually using a stirring rod until it hardens. Next, the gel was put in an oven for drying process. Drying aims for the auto-combustion process. The gel was heated at 150^0C for 1 hour. The sample that was originally in the form of a gel will turn into powder. The powdered sample was crushed using mortar to reduce the particle size and make it mode homogenious. Then the particle was annealed in a furnance at 500^0C for 4 hours. The annealed sample was then crushed using mortar. The above procedure was repeated preparation of Ni-doped $CoFe_2O_4$ NPs by simple

adding Nickel nitrate to the solution preparation at different wt%. The characterizations were carried out using XRD, FTIR, SEM, VSM, and UV-Vis.

3. Results and discussion

This research focused on analyzing the characteristics of $CoFe_2O_4$ -doped Nickel. XRD was carried out in order to determine the crystal structure. FTIR was carried out to identify the absorption peaks. SEM was conducted to determine the morphological structure. VSM was used to analyze the magnetic properties and UV-Vis was used to analyze the photocatalytic performance of the sample

3.1. X-Ray Diffraction (XRD)

X-Ray Diffraction (XRD) was carried out to confirm the type of phase formed from the material, such as crystal properties, lattice parameters, crystal structure, and also the polycrystalline phase [4]. **FIGURE 1** shows the XRD pattern of the as prepared samples named as $Ni_xCo_{(1-x)}Fe_2O_4$ (x = 0 wt%, 2 wt%, 4 wt%, 6 wt%, 8 wt%, and 10 wt%). The diffraction pattern was analyzed using Origin software.

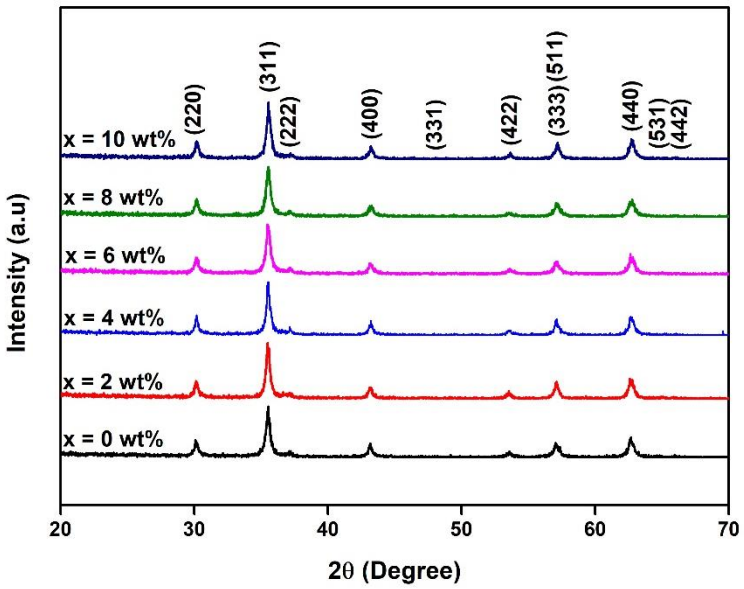

FIGURE 1. The XRD pattern of Ni-doped $CoFe_2O_4$ NPs

The peaks observed respected to the planes (220), (311), (222), (400), (331), (422), (333), (511), (440), (531), and (442). All of the samples have the same peak so that it can be seen that the sample is consistent and has a single phase. The peaks for corresponding 2θ values confirm that the sample has a spinel-type FCC structure belongs to the space group *Fd3m.* XRD results were analyzed using Fullprof with the Rietveld refinement method. The XRD results were shown in **TABLE 1**. Based on the **TABLE 1**. It is noticed that the lattice parameter decreased with increasing nickel ions content. This is due to the smaller ionic radius nickel ions (0.63Å) replaced the cobalt ions (0.78Å) site. This results are accordance with the research of [4], [11], [12] where there is a decrease in lattice parameters along with the addition of nickel content. In addition, it is also obtained that the density value is increasing and the interplanar distance is decreasing along with the increase in nickel content[4]. The 3D shape of the crystal structure of each sample using Vesta software were shown in **FIGURE 2**

TABLE 1. The XRD results pattern of Ni-doped $CoFe_2O_4$ NPs

	$Ni_xCo_{(1-X)}Fe_2O_4$					
	x = 0wt%	**x = 2wt%**	**x = 4wt%**	**x = 6wt%**	**x = 8wt%**	**x = 10wt%**
Crystal system	Cubic	Cubic	Cubic	Cubic	Cubic	Cubic
Space group	Fd-3m	Fd-3m	Fd-3m	Fd-3m	Fd-3m	Fd-3m
Peak Position (2θ)	35.55	35.59	35.52	35.54	35.52	35.52
FWHM	0.29	0.33	0.25	0.44	0.31	0.39
Lattice parameter (a = b = c) (Å)	8.3795	8.3797	8.3762	8.3773	8.3742	8.3732
$\alpha = \beta = \gamma$	90	90	90	90	90	90
Volume (Å^3)	588.3824	588.4383	587.6803	587.9189	587.2680	587.0425
Density	5.297 g/cm^3	5.297 g/cm^3	5.303 g/cm^3	5.305 g/cm^3	5.307 g/cm^3	5.398 g/cm^3
R_{Bragg}	8.81	22.5	21.7	16.90	17.01	18.90
R_f(%)	7.87	16.1	16.6	13.20	12.10	14.50
$d_{spacing}$ (Å)	2.5265	2.5265	2.5255	2.5258	2.5249	2.5246
Crystalite size (nm)	28,6138	24.36	25.62	16,2312	22,1512	21,6688
G.O.F (χ^2)	0.74	1.2	1.2	1.2	1.1	1.7

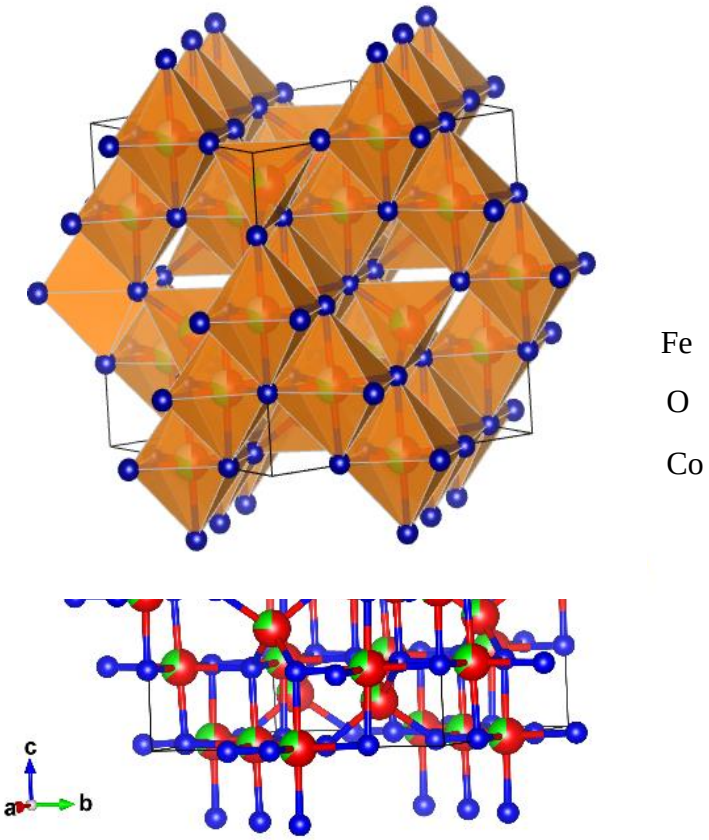

FIGURE 2. The 3D Shape of Ni-doped $CoFe_2O_4$ NPs

3.2. Fourier Transform InfraRed (FTIR)

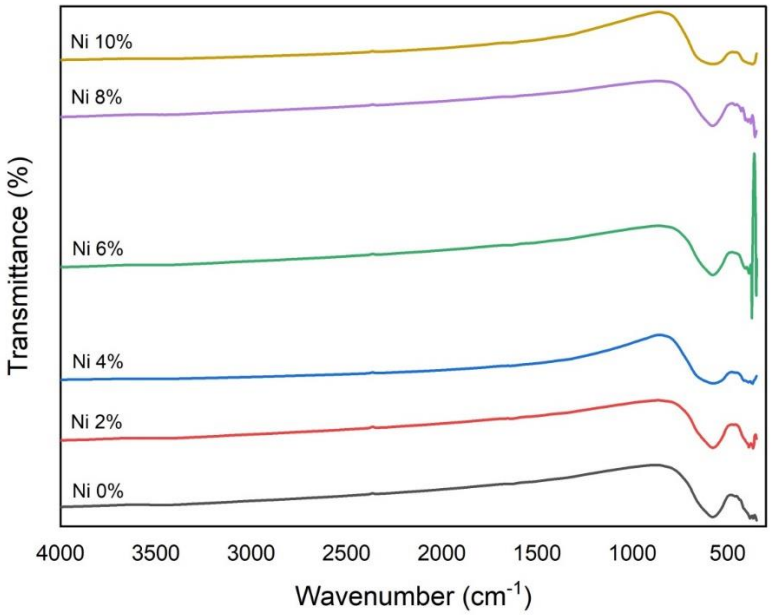

FIGURE 3. The FTIR spectrum Pattern of Ni-doped $CoFe_2O_4$ NPs

The results of these absorption peaks were compared with those of [4] and [5] to determine the functional groups formed. Based on the FTIR data, it is known that all samples show octahedral and tetrahedral sites. This is in accordance with the main characteristic of the configuration of the ferrite spinel which consists of octahedral and tetrahedral sites. The FTIR results also show a tetrahedral shift towards higher frequencies along with the addition of Ni content. These results are caused by the placement of Ni2+ ions at the octahedral site and forcing Fe3+ to go to the tetrahedral site so that Fe ions with a lower atomic mass replace Co at the tetrahedral site [4]. These results also show changes in the distribution of Fe at both sites. In addition, the FTIR results have peaks indicating H-O-H bonds. This peak is shown in small intensity. H-O-H bonds formed on the surface of the sample caused by the long period of time between the annealing process and the characterization process.

3.3. Scanning Electron Microscopy (SEM)

SEM is used to determine the surface morphology and shape of the material [13]. This test produces surface images of the Co(1-X)NixFe2O4 material that has been made. SEM results are displayed with a magnification of 50,000 times. **FIGURE 4** is an image of the Scanning Electron Micrography (SEM) test results of the $Ni_xCo_{(1-x)}Fe_2O_4$ (x = 0 wt%, 2 wt%, 4 wt%, 6 wt%, 8 wt%, and 10 wt%). SEM is one of the effective methods used to analyze materials at the micrometer to nanometer scale [14]. The SEM images were displayed in **FIGURE 4.** (a, b, c, d, e, & f). It shows that the particles get agglomerates and show irregularity in all of samples. Agglomeration occurs during the material synthesis process and is caused by the use of low annealing temperatures. From the SEM results, it is also known that the particle size tends to get smaller with the addition of Ni content.

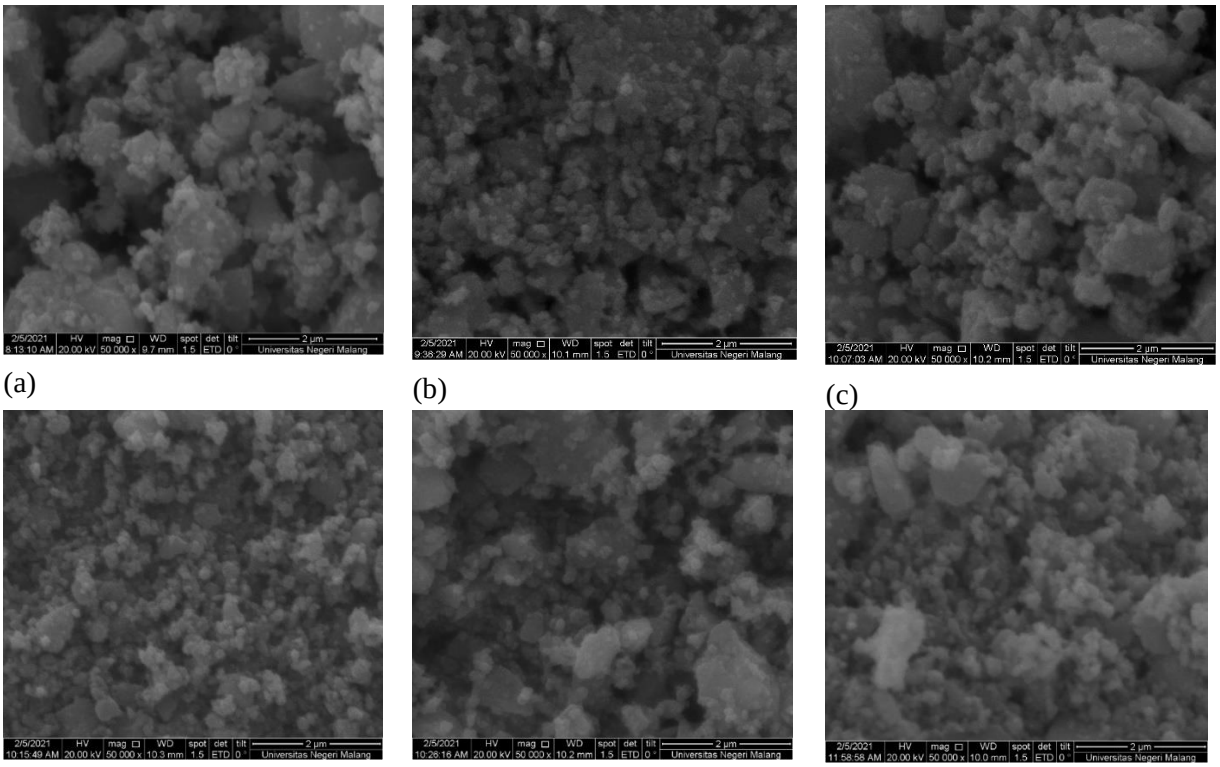

FIGURE 4. SEM images of $Ni_xCo_{(1-x)}Fe_2O_4$ (a) x = 0 wt%, (b) 2 wt%, (c) 4 wt%,(d) 6 wt%, (e) 8 wt%, and (f) 10 wt%

3.4. Magnetic Study

Room temperature magnetic study (M-H curves) shown in **FIGURE 5.** M-H curve indicates that saturation magnetization tends to decrease when doping concentration of nickel varies 0 wt% to 6 wt %. Decreasing of saturation magnetization depends upon the two factors: (1) interaction of magnetic ions and magnetic interactions with the external applied field determines the net magnetic moment of the material and (2) being a non-magnetic ion [15]. The coercivity value of the samples also decreased with increasing nickel doping. The decrease in the magnetic properties of the sample indicates that the pulled of the sample from the liquid material will be more difficult to do as the doping increases. This is also supported by the smaller crystal size and particle size in the sample which will be inversely proportional to the ability to reuse through an external magnetic field.

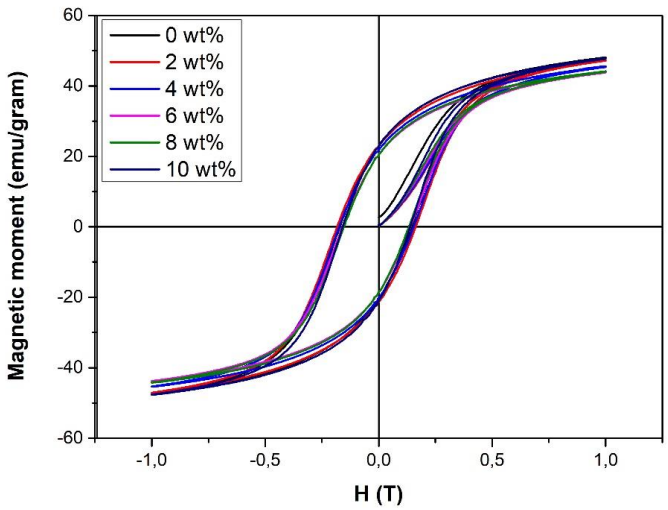

FIGURE 5. M-H hysteresis loops of different samples

3.5. Photocatalytic Performance

The optical properties of $Ni_xCo_{(1-x)}Fe_2O_4$ (x = 0 wt%, 2 wt%, 4 wt%, 6 wt%, 8 wt%, and 10 wt) were investigated using UV – Spectroscopy in the wavelength range of 400 – 800 nm shown in **FIGURE 6**. A number of factors that usually affect absorbance are the center of impurities, grain size, bandgap, lattice parameters, and surface roughness.

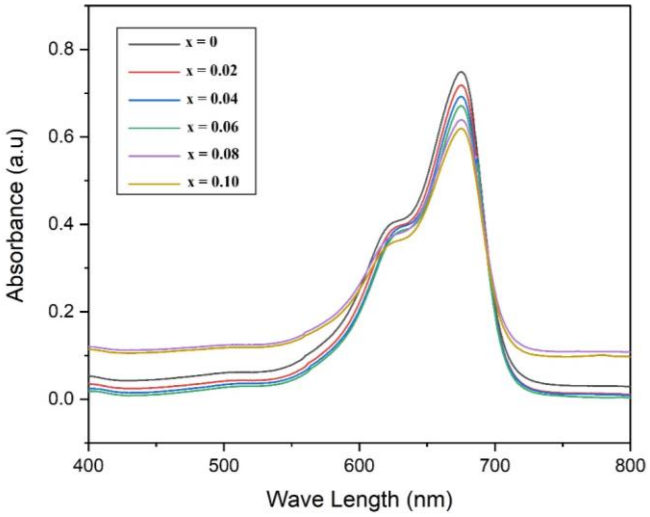

(a)

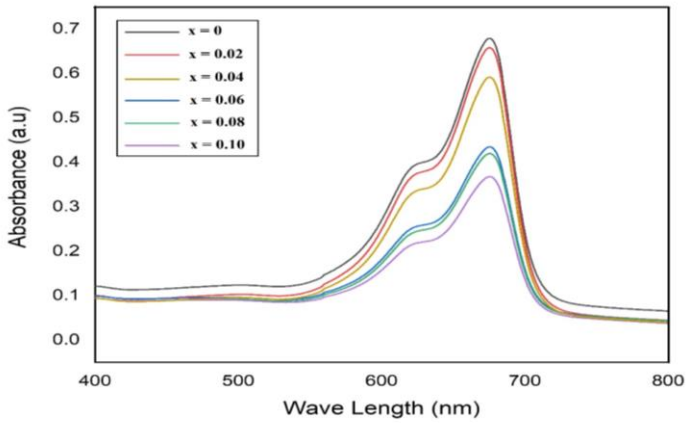

(b)

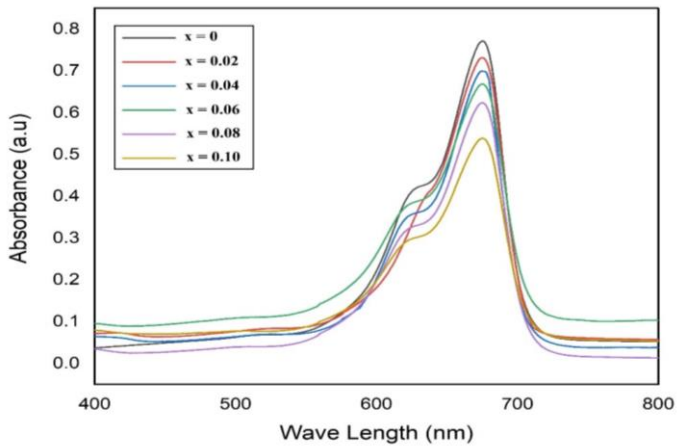

(c)

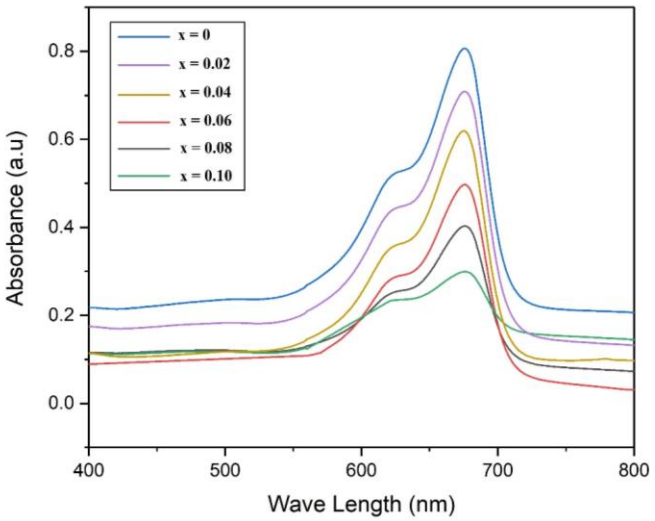

(d)

FIGURE 6. Graph of UV-Vis Test Results (a) without irradiation (b) 2 minutes (c) 5 minutes (d) 10 minutes

From the result, the absorbance peak of $Co_{(1-x)}Ni_xFe_2O_4$ nanoparticles with 0% concentration was at the top and then decreased from 2 wt%, 4 wt%, 6 wt%, 8 wt%, and 10 wt% concentrations. This proves that the effect of doping concentration will cause a reduction in absorbance. So from the UV-Vis test results for $Co_{(1-x)}Ni_xFe_2O_4$ nanoparticles, the higher the doping, the lower the absorbance value, resulting in better catalyst capabilities. The effect of doping will affect the results of the UV-vis test by looking at the size of the resulting crystal. The smaller the crystal size produced by nickel-doped cobalt ferrite nanoparticles, the lower the absorbance value produced will result in better UV-Vis results [4].

4. Conclusion

XRD pattern analysis showed a decrease in lattice parameters, an increase in density, and a decrease in interplanar distance along with the addition of Nickel content in Cobalt Ferrite nanoparticles. In addition, there is also a shift in the peak in the sample along with the addition of Nickel content in the sample. FTIR results show that the sample has functional groups at octahedral and tetrahedral sites. This is in accordance with the main characteristic of the configuration of the ferrite spinel which consists of octahedral and tetrahedral sites. In the image of the SEM test results, it is known that clumping and irregularities occur in all samples. In addition, the photocatalytic performance of cobalt ferrite-doped nickel stated that there was an increase in the degradation of methylene blue dye along with the increase in sample irradiation time. it is also seen that the photocatalyst performance increases with the addition of nickel.

Acknowledgement

This research was funded by DIPA of Universitas Sebelas Maret of The Republic of Indonesia (Penelitian Unggulan Universitas Sebelas Maret Contract No. 260/UN27.22/HK.07.00/2021)

References

[1] D. Mehta, S. Mazumdar, and S. K. Singh, "Magnetic adsorbents for the treatment of water/wastewater-A review," *J. Water Process Eng.*, vol. 7, pp. 244–265, 2015, doi: 10.1016/j.jwpe.2015.07.001.

[2] O. Arnop, B. Budiyanto, and R. Saefuddin, "Kajian Evaluasi Mutu Sungai Nelas Dengan Metode Storet Dan Indeks Pencemaran," *Nat. J. Penelit. Pengelolaan Sumber Daya Alam dan Lingkung.*, vol. 8, no. 1, pp. 15–24, 2019, doi: 10.31186/naturalis.8.1.9158.

[3] P. Singh *et al.*, "Systematic review on applicability of magnetic iron oxides–integrated photocatalysts for degradation of organic pollutants in water," *Mater. Today Chem.*, vol. 14, 2019, doi: 10.1016/j.mtchem.2019.08.005.

[4] J. Revathi, M. J. Abel, V. Archana, T. Sumithra, R. Thiruneelakandan, and J. Joseph prince, "Synthesis and characterization of CoFe2O4 and Ni-doped CoFe2O4 nanoparticles by chemical Co-precipitation technique for photo-degradation of organic dyestuffs under direct sunlight," *Phys. B Condens. Matter*, vol. 587, no. October 2019, p. 412136, 2020, doi: 10.1016/j.physb.2020.412136.

[5] L. Kumar, P. Kumar, A. Narayan, and M. Kar, "Rietveld analysis of XRD patterns of different sizes of nanocrystalline cobalt ferrite," *Int. Nano Lett.*, vol. 3, no. 1, pp. 1–12, 2013, doi: 10.1186/2228-5326-3-8.

[6] Q. Song and Z. J. Zhang, "Shape Control and Associated Magnetic Properties of Spinel Cobalt Ferrite Nanocrystals," *J. Am. Chem. Soc.*, vol. 126, no. 19, pp. 6164–6168, 2004, doi: 10.1021/ja049931r.

[7] S. Dong *et al.*, "Recent developments in heterogeneous photocatalytic water treatment using visible light-responsive photocatalysts: A review," *RSC Adv.*, vol. 5, no. 19, pp. 14610–14630, 2015, doi: 10.1039/c4ra13734e.

[8] A. Licciulli and D. Lisi, *Self-Cleaning Glass*. Universita Degli Studi di Lecce, 2002.

[9] S. Singh and S. Singhal, "Transition metal doped cobalt ferrite nanoparticles: Efficient photocatalyst for photodegradation of textile dye," *Mater. Today Proc.*, vol. 14, pp. 453–460, 2019, doi: 10.1016/j.matpr.2019.04.168.

[10] A. Lassoued and J. F. Li, "Magnetic and photocatalytic properties of Ni–Co ferrites," *Solid State Sci.*, vol. 104, no. April, 2020, doi: 10.1016/j.solidstatesciences.2020.106199.

[11] A. Kumar, P. Sharma, and D. Varshney, "Structural, vibrational and dielectric study of Ni doped spinel Co ferrites: Co1-xNixFe2O4 (x=0.0, 0.5, 1.0)," *Ceram. Int.*, vol. 40, no. 8 PART B, pp. 12855–12860, 2014, doi: 10.1016/j.ceramint.2014.04.140.

[12] S. S. Bharambe, A. Trimukhe, and P. Bhatia, "Synthesis Techniques of Nickel Substituted Cobalt Ferrites-An Investigative Study Using Structural Data," *Mater. Today Proc.*, vol. 23, pp. 373–381, 2020, doi: 10.1016/j.matpr.2020.02.056.

[13] P. P. Hankare, K. R. Sanadi, K. M. Garadkar, D. R. Patil, and I. S. Mulla, "Synthesis and characterization of nickel substituted cobalt ferrite nanoparticles by sol-gel auto-combustion method," *J. Alloys Compd.*, vol. 553, pp. 383–388, 2013, doi: 10.1016/j.jallcom.2012.11.181.

[14] A. Mohammed, "Scanning electron microscopy (SEM): A review," no. December, 2018.

[15] S. Chakrabarty, A. Dutta, and M. Pal, "Effect of yttrium doping on structure, magnetic and electrical properties of nanocrystalline cobalt ferrite," *J. Magn. Magn. Mater.*, vol. 461, pp. 69–75, 2018, doi: 10.1016/j.jmmm.2018.04.051.